International Journal for Housing Science and Its Applications
Publish August 10, 2025. Volume 46, Issue 4 Pages 3810-3820

https://doi.org/10.70517/ijhsa464503a

Study on the stress performance of key nodes of Rigid-Frame Bridge based on variational method and its optimized design

Fengwu Yu[1], Shuai Guo[1], Jun Tang[1] and Chuanyang Yang[1,*]
[1] CCCC First Highway Engineering Group Co., Ltd., Beijing, 100000, China
Corresponding authors: (e-mail: 18587427119@163.com).

Abstract Rigid-frame bridges are widely used in engineering due to their good integrity and reasonable pier and beam consolidation force performance. In this study, the energy variational method is introduced into the solution of shear hysteresis coefficient of Rigid-Frame Bridge, by analyzing the strain energy of each part of Rigid-Frame Bridge under the action of load, in order to calculate the shear hysteresis coefficient of Rigid-Frame Bridge, and then analyze the force performance of Rigid-Frame Bridge. Based on the ANSYS program and the force analysis method, a finite element simulation model of Rigid-Frame Bridge is constructed. The results of the study show that when all lanes and sidewalks of Rigid-Frame Bridge are loaded, the maximum bending positive stresses in the top and bottom plates of the J1 section at the critical node are -21.42 MPa and -24.81 MPa, respectively, and the maximum shear hysteresis coefficients of the top and bottom plates of the steel bridge in the J2 section are 1.50 and 8.01, respectively. In addition, the maximum shear hysteresis coefficients of the top plates of J1 and J2 sections show a gradual decreasing trend when the tilt of the web plate of Rigid-Frame Bridge is changed from 90° to 60° and 45°, so it can be considered to increase the tilt of the web plate of Rigid-Frame Bridge to achieve the optimization of the structural design and safety of Rigid-Frame Bridge. The research results of this paper can provide scientific basis and technical guidance for the formulation of relevant specifications and engineering design of Rigid-Frame Bridges, which can help optimize the structure of this type of bridges and have good social and economic benefits.

Index Terms variational method, shear lag coefficient, ANSYS, Rigid-Frame Bridges, force analysis, structural design

I. Introduction

Rigid-frame bridge is a form of bridge with rigid structure, which is characterized by the rigidity of the connection points between the members in the bridge structure, which can resist the action of external forces and maintain the stability and stiffness of the structure. The force characteristics of Rigid-Frame Bridge are characterized by the uniform distribution of forces [1]-[4]. In the structure of Rigid-Frame Bridge, the connection points between the members are rigidly connected, so that the external force can be uniformly transmitted to the whole bridge structure. This type of force can make the bridge structure share the force uniformly when it is subjected to the external force, avoiding the local members to be subjected to excessive force and lead to the destruction of the structure [5]-[8].

As an important part of the whole structure, the nodes of Rigid-Frame Bridge structure have a crucial influence on the overall performance, stiffness and stability of the structure. Rigid bridge structure node optimization refers to improve the performance and reliability of the nodes through the optimization and improvement of the node design, material selection, manufacturing process and construction quality [9]-[12]. It specifically includes the following aspects. First, the optimization of node structure, through the optimization of node structure, to reduce the phenomena such as stress concentration and crack extension in the nodes, and improve the seismic capacity and bearing capacity of the nodes [13]-[15]. The second is the optimization of materials, through the use of high-strength steel materials, reasonable selection of the thickness and hardness of steel materials, etc., to improve the strength and toughness of nodes [16], [17]. Third, the optimization of manufacturing process, through the optimization of manufacturing process, such as the use of pre-embedded parts, on-site welding, machining, etc., to improve the manufacturing quality and performance of nodes [18], [19]. The fourth is the optimization of construction quality, through strengthening construction supervision and on-site management, controlling the construction quality and process requirements to ensure the reasonableness, tightness and completeness of node construction [20], [21].

This paper applies the energy variational method to solve the shear hysteresis effect of Rigid-Frame Bridges, proposes a simple, effective and innovative calculation method of the shear hysteresis effect of bridges, and analyzes the force performance and optimization design direction of Rigid-Frame Bridges based on this method.

First, the shear lag coefficient is introduced to realize the simple description of the shear lag effect of Rigid-Frame Bridges, and the bridge flange plate and effective distribution width are analyzed. Then, according to the principle of minimum potential energy of energy partitioning method, the solution method of deformation potential energy such as web strain energy, upper and lower flange strain energy, etc. under symmetric longitudinal bending load is proposed, and the shear hysteresis coefficients of Rigid-Frame Bridges are obtained by combining with calculations. Based on this, an adaptive finite element simulation model of Rigid-Frame Bridge is constructed in ANSYS program. In this study, a Rigid-Frame Bridge is taken as an engineering example, and the validity of the finite element model is verified, and the force performance of the key nodes of Rigid-Frame Bridge is simulated and analyzed. It also explores the influence of web inclination on the shear hysteresis effect of the bridge, which provides a reference strategy for the optimized design of Rigid-Frame Bridges.

II. Method

II. A. Stress test methods for Rigid-Frame Bridges

Stress monitoring of Rigid-Frame Bridge structures is usually carried out by measuring the strain of the structure through sensors and then back-calculating the stress results through the elastic modulus of the material. At present, the mainstream sensors in bridge engineering include mechanical strain tester, resistance strain gauge, steel string strain gauge, fiber grating strain gauge and so on. Combined with the structural and construction characteristics of large-span continuous Rigid-Frame Bridges, steel string strain gauges are widely used in the stress monitoring and control process.

The steel string strain gauge reflects the change of steel string force through the change of steel string vibration frequency. Since the steel string is set in a steel sealed cylinder and isolated from the outside world, it has strong anti-interference ability and high measurement accuracy. The vibration of the steel string depends on the external pulse excitation, and the output is the numerical characteristic signal of vibration frequency, which is easy to read the data. According to the mass density of the steel string, length and output of the self-oscillation frequency, can quickly calculate the tension of the steel string. The formula for calculating the tension applied is as follows:

$$T = 4\rho A l^2 f^2 \tag{1}$$

where T is the tension applied to the string (N), l is the length of the string (m), ρA is the mass density of the string (kg/m), and f represents the frequency of self-oscillation of the string (Hz).

The strain is then obtained:

$$\varepsilon_g = \frac{\sigma_g}{E_g} = \frac{4\rho l^2 f^2}{E_g} \tag{2}$$

where E_g is the modulus of elasticity of the chord, σ is the tensile stress on the chord, and ε is the strain on the chord.

When the construction proceeds to the stress control section, the steel string strain gauges are fixed to the reinforcement network of the section, and care should be taken to ensure that the length of the strings is oriented in the same direction as the stresses to be measured. After pouring the section concrete and waiting for it to set, the strain gauges facilitate the concrete to form a single unit. When strain occurs in the concrete, the two pivot points of the steel strings in the strain gauge are then displaced by an equal amount, thus changing the tension on the strings, which is reflected by the change in the self-oscillation frequency. For the calculation, it is assumed that the mass density of the string wire is constant only the change of tension and length is considered. There is no relative displacement between the strain gauge and the concrete, so the strain occurring in the concrete is equal to the strain increment in the steel string, which is calculated by the following equation:

$$\varepsilon_c = \frac{4\rho l^2 f^2}{Eg} - \varepsilon_{g0} \tag{3}$$

where ε_{g0} is the initial strain of the string wire and ε_c is the strain occurring in the concrete.

Based on the elastic modulus of the concrete, the stress of the concrete in the area where the sensor is located can be calculated by the stress-strain equation:

$$\sigma_c = E_c \cdot \varepsilon_c \tag{4}$$

where E_c is the modulus of elasticity of the concrete material and σ_c is the internal stress in the concrete at the location of the strain gauge.

II. B. Variational Method Based Shear Hysteresis Analysis of Rigid Bridge

II. B. 1) Shear lag parameters

(1) Shear lag coefficient λ

In order to describe the shear lag effect of Rigid-Frame Bridges [22] more concisely, the concept of shear lag coefficient λ [23] is introduced:

$$\lambda = \frac{\text{Consider the normal stress of shear deformation (upper and lower plates)}}{\text{The normal stress is obtained according to the elementary beam theory}} \tag{5}$$

Shear hysteresis coefficient λ is the main parameter describing the shear hysteresis effect of a Rigid-Frame Bridge girder.

(2) The effectiveness of the loads carried by the flange plates e

If P denotes the sum of forces carried by the top plate of any box girder section:

$$P = 2t_2 \int_0^{\frac{b}{2}} \sigma_x dy = 2t_2 \left(ED \frac{\pi}{2l} \cos \frac{\pi x}{2l} \right) \left(\frac{2nl}{\pi} \right) sh \frac{\pi b}{4nl} \tag{6}$$

If the shear lag effect is not considered, the force on the top plate is:

$$P_1 = \sigma_x t_2 b = t_2 bED \frac{\pi}{2l} \cos \frac{\pi x}{2l} ch \frac{\pi b}{4nl} \tag{7}$$

$$e = \frac{P}{P_1} = \frac{4nl}{\pi b} th \frac{\pi b}{4nl} \tag{8}$$

where e is the effectiveness of the flange to withstand the load, b is the actual width of the flange, t_2 is the thickness of the flange, l is the span of the beam, and σ_x is the tensile or compressive stress of the beam. In the above equation, e is the effectiveness of the flange to withstand the load, and its magnitude indicates the magnitude of the shear lag and the degree of change.

(3) Effective distribution width of box girder b_c

It is complicated to analyze the uneven distribution law of the flange stresses by using the exact theory, especially it is not easy to be applied in engineering design. In order to utilize the simple primary beam theoretical formulas, but also close to the maximum value of the actual stress in the flange, the concept of “effective distribution width of the flange” has been proposed. Its mathematical expression is:

$$b_c = \frac{t \int_0^b \sigma(x, y) dy}{t \sigma_{\max}} \tag{9}$$

where b_c is the effective distribution width of the flange, b is the actual width of the flange, t is the thickness of the flange, x is the coordinate along the span length direction, and y is the coordinate along the cross-section width direction. From the above equation, it can be seen that the effective distribution width of the flange is converted according to the principle that the volume of internal stress in the flange is equal to the volume of internal stress in the flange of the converted section. The ratio of the effective width to the actual width is called the effective width ratio, which reflects the degree of non-uniformity of the stress distribution of the airfoil. Therefore, the engineering design should use this discounted section flexural modulus, according to the primary beam bending theory to calculate its longitudinal bending stress and deflection.

II. B. 2) Methods for solving the shear lag effect

For the study of shear lag effect, related scholars have done a lot of theoretical and experimental research work, especially for equal cross-section box girders, and a lot of progress has been made. However, for the calculation method of shear lagging effect for variable cross-section box girders, it is very difficult to solve the exact solution due to the system of ordinary differential equations with variable coefficients. In this paper, the energy variational method [24] is applied to the shear lag analysis of box girders with Rigid-Frame Bridge cross section to provide a simple and effective calculation method for engineering calculation and design.

The box girder of Rigid-Frame Bridge is a space structure, and the force analysis is very complicated. At present, in the engineering design at home and abroad, the load decomposition analysis method is usually used to analyze the structure according to the thin-walled rod theory, i.e., the vertical load acting on the top surface of the box girder at any position is decomposed into symmetric longitudinal bending load, anti-symmetric torsion load, and distortion load of three kinds of equivalent load, and then superimposed to get the final solution. This paper investigates the first load case, i.e., the shear hysteresis problem under symmetric longitudinal bending load.

The box girder in symmetric deflection, the upper and lower flanges no longer conform to the flat section assumption because of shear deformation, introducing two generalized displacements, the vertical deflection of the girder denoted by ω and the longitudinal displacement of the girder described by $u(x, y)$. Therefore, there is:

$$\left.\begin{aligned}\omega &= \omega(x)\\ u(x,y) &= Z_{\text{Up (down)}}\left[\frac{d\omega}{dx}+\left(1-\frac{y^m}{(\xi_i b)^m}\right)\cdot u(x)\right]\end{aligned}\right\} \tag{10}$$

where $u(x,y)$ is the longitudinal displacement of the beam, $u(x)$ is the maximum difference of the shear angle, b is half of the net width of the box chamber, $Z_{\text{Up (down)}}$ is the distance of the middle surface of the upper and lower wing plates from the center axis of the box girder, m is the displacement function $u(x,y)$ along the y direction of the m parabolic distribution.

The vertical extrusion ξ_x of the upper and lower wing plates, the out-of-plane shear deformation γ_{xz},γ_{yz} and the transverse bending and transverse strain are all trace and negligible. In addition, because ξ_1,ξ_2,ξ_3 not the same, the top plate, cantilever part and bottom plate should have different $u(x)$ expressions, if still use the uniform $u(x)$ expression, the introduction of correction coefficients with shear angle difference, that is:

$$u_i(x,y) = \mp Z_{\text{Up (down)}}\left\{\frac{\mathrm{d}\omega}{\mathrm{d}x}+\zeta_i\left[1-\frac{y^m}{(\xi_i b)^m}\right]u(x)\right\} \tag{11}$$

where, $\zeta_i = \eta\dfrac{\xi_i}{\xi_{\max}}$ is the correction coefficient considering the width of inner and outer flange plate and boundary conditions.

According to the principle of minimum potential energy, under the action of the external force, in a stable equilibrium state of the cardinal body, in all the displacements to meet the boundary conditions, there is actually a group of displacements that can make the whole system of the total potential energy for the minimum, the total potential energy of the system of the first-order variation is zero:

$$\delta_\pi = \delta(\overline{V}-\overline{W}) \tag{12}$$

where, $\overline{v}$ is the strain energy in the structural system; $\overline{w}$ is the external potential energy.

When the box girder bends, the external load potential energy:

$$\overline{W} = -\int_0^l M(x)\frac{d^2\omega}{dx^2}dx \tag{13}$$

The potential energy of each deformation of the beam is calculated as follows.

Web Strain Energy:

$$\overline{V_w} = \frac{1}{2}\int_0^l EI_w\left(\frac{d^2\omega}{dx^2}\right)^2 dx \tag{14}$$

where I_w is the moment of inertia of the web against the center of section form.

Upper and lower wing plate strain energy:

$$\begin{aligned}\overline{V_{su}} &= \overline{V_{su1}}+\overline{V_{su2}}(\text{Upper wing})\\ &= 2\left\{\frac{1}{2}\int_0^l\int_0^{\xi_1 b} t_{u1}(E\varepsilon_{xu1}^2+G\gamma_{u1}^2)dxdy+\frac{1}{2}\int_0^l\int_0^{\xi_2 b} t_{u2}(E\varepsilon_{xu2}^2+G\gamma_{u2}^2)dxdy\right\}\end{aligned} \tag{15}$$

$$\overline{V_{sb}} = 2\left\{\frac{1}{2}\int_0^l\int_0^{\xi_3 b} t_b(E\varepsilon_{xb}^2+G\gamma_b^2)dxdy\right\}(\text{Lower wing}) \tag{16}$$

where t_{u1},t_{u2},t_b is the thickness of the airfoil at the corresponding position in the upper and lower airfoils, respectively.

The total potential energy of the system:

$$\pi = \overline{V_{su1}}+\overline{V_{su2}}+\overline{V_{sb}}+\overline{V_w}-\overline{W} \tag{17}$$

II. C.Adaptive finite element simulation and analysis model construction

The first thing to do for the key node stress performance analysis of Rigid-Frame Bridge is to simulate the bridge structure of Rigid-Frame Bridge, the simulation analysis of the bridge structure is through the finite element software according to the design drawings of the bridge for modeling, and then extract the main girder pre-arch as well as each section of the bridge line and control section stresses, etc. From the software, the main girder pre-arch and the bridge line and control cross-section stresses are extracted. Combined with the characteristics of Rigid-Frame Bridge, which is the object of study in this paper, a series of simulation and analysis are completed by ANSYS program [25]. ANSYS is an advanced structural analysis software, in the building analysis, the software for the

structure of the various characteristics of the comprehensive consideration, and recorded domestic and foreign civil engineering specifications, in line with the habit of the domestic structural calculations of bridge structures in the cable-stayed bridges, continuous girder bridge, continuous Rigid-Frame Bridge, suspension bridge, and bridge structure, and the structural calculation of bridge structure, in the case of cable-stayed bridges, continuous girder bridge, continuous Rigid-Frame Bridge, suspension bridge and bridge structure. It is widely used in the simulation calculation of various bridge types such as cable-stayed bridge, continuous Rigid-Frame Bridge and suspension bridge.

The accuracy of the mesh in finite element calculation is directly related to the accuracy of the calculation results, and the adaptive finite element method is a numerical method that can automatically adjust the mesh division to improve the solution process through adaptive analysis. It uses the finite element calculation results to construct the error estimation formula, uses the error estimation formula to calculate the error distribution in each region, and automatically encrypts the mesh in the place of large error to achieve the purpose of obtaining high calculation accuracy with less workload, which is a calculation method with high efficiency and high reliability. The ANSYS program is able to automatically estimate the error brought about by mesh partitioning in a specific type of analysis. Through this error estimation, the program can determine if the mesh is fine enough. If it is not, the program will automatically refine the mesh to reduce the error. This process of automatically estimating meshing errors and refining the mesh is called adaptive meshing.

The basic process of performing adaptive meshing and analysis consists of the following steps.

(1) Specify the cell type, real constants and material properties. So these have to fulfill the prerequisites described earlier.

(2) Create a geometric model. The user does not need to specify the cell size nor mesh, the ADAPT macro will automatically mesh.

(3) Specify the analysis type, analysis options, loads, and load step options in /PREP7 or /SOLU. Apply only solid model loads and inertial loads in one load step, constraint equations, and multiple load steps can be added through the ADATPSOL.MAC user subroutine.

(4) Activate the ADAPT macro in /SOLU or in the initial state. During the iterations of adaptive meshing, the cell size will be adjusted to reduce or increase the cell energy error until the error meets the specified numerical requirements.

(5) After the convergence of the adaptive meshing computation, it enters the post-processing.

In ANSYS, it is very convenient to add loads for Rigid-Frame Bridge models. Different loads such as static load, dynamic load, temperature load and prestress have different load adding modules, and the load weight coefficients can be set according to the relevant norms to carry out different load combinations. After the loads are added, the size of the loads on each unit and node can be displayed in a table, and the load values can be modified directly in the table, which can be used to modify the load conditions of the model at any time. ANSYS provides a variety of ways to query the calculation results. For static analysis, the deformation and stress values of the key nodes of Rigid-Frame Bridge can be directly displayed on the model, and the result table can also be generated and directly copied to the Excel table, which is convenient to extract. When performing dynamic analysis, a major feature of the software is the function of moving load tracker, through which the internal force and displacement values of the structure can be obtained when the moving load is in different action positions, so as to find the most unfavorable position of the load, which provides a great help for the optimal design of rigid-frame bridges.

III. Results and discussion

III. A. Validation of Finite Element Model Validity

III. A. 1) Overview of project examples

The research object selected for this paper is a frame continuous Rigid-Frame Bridge, this bridge is 65m+100m+65m 3-span prestressed continuous Rigid-Frame Bridge, bidirectional six-lane design, the lateral two widths are arranged symmetrically according to the bridge centerline. The total width of the bridge is 30m, the main girder is single box single chamber box girder, the top width of single box girder is 14.25m, the bottom width is 8.5m, the length of cantilever is 3.50m, the girder height of the middle (side) span is changed from the middle of the span is 2.5m to the root is 5.5m, and the change of the beam's bottom edge is set up according to the round curve. The top plate of box girder is 0.35m thick, the bottom plate changes from 0.35m thick in the span to 0.8m at the root, and the thickness of the web plate is 0.45m and 0.70m respectively. The main girder adopts C50 concrete, and arranges longitudinal, transverse and vertical prestressing. The longitudinal direction adopts OVM15-12(7φ5) anchorage system, and the transverse direction adopts OVM15BM-3(7φ5) anchorage system, and the standard strength of 7φ5 steel hinge R_y=1950MPa, and the control stress σ_k=1423MPa. The vertical direction adopts the cold-drawn Ⅳ Φ 32 anchorage system, and the tensile strength of Ⅳ Φ 32 rebar R_y=775MPa, and the control

stress σ_k =653.2MPa. The main pier is 8m×5.5m double thin-walled hollow pier, with heights of 35.62m and 34.26m, using C40 concrete. The weld joints of Rigid-Frame Bridge are passed through the weld holes and then sealed with sealant. In order to facilitate the daily maintenance and repair of this Rigid-Frame Bridge, an access tunnel is arranged at the bottom plate of the box girder close to the end pivot diaphragm. The bridge deck pavement layer is 185mm thick, and the anti-collision guardrail is made of steel raw material. Bridge support at the outer web of the steel box needs to be set seismic rubber block, rubber size 750 × 750 × 60mm, for natural rubber, through the bolts connected to the side wall of the steel box. Construction should be the first rubber plate in place, and then set up the mold construction cover beam block. The bridge bearing uses shock-absorbing basin-type bearing, and the horizontal bearing capacity of the non-slip direction of the shock-absorbing type bearing is greater than or equal to 25% of the vertical bearing capacity of the bearing.

III. A. 2) Model validation

The continuous rigid frame bridge was load tested after completion, and a part of the results of the static load test in the inspection report was taken to compare with the simulation results obtained from the finite element simulation in this paper to verify the accuracy of the model. According to the inspection report of Rigid-Frame Bridge, 21 stress test sections were arranged in the whole bridge for the static load test (one test section was arranged every 11.5m along the longitudinal span length). The strain value of each section is detected by strain gauges and strain gauges, and then the stress value of each test point is converted according to the modulus of elasticity of the material. Take one loading condition in the test, i.e. arrange a pair of equivalent loads symmetrical to the beam ribs in the mid-span (the equivalent loading is carried out by the loading truck in the test, and according to the general specification for highway bridge and culvert design, take the standard value of highway -class Ⅰ lane load centralized load as 360KN), add the same form of load to the finite element model, and then add the stress value of the center of the top plate of each test cross-section in the test report with the stress value of the corresponding position obtained from the finite element simulation. Comparing the stress value at the top plate center of each test section in the test report with the stress value at the corresponding position obtained by finite element simulation, the results of the stress test and finite element simulation of the key nodes of Rigid-Frame Bridge are shown in Table 1. The distribution trends of the calculated and measured values are relatively consistent, with most of the values ranging from 1.38% to 18.46% (15 measurement points). The absolute value of the measured stress values at 11 of all measurement points is greater than the finite element calculated stress values, which may be due to the fact that the weight of materials such as concrete and asphalt on the steel bridge deck was neglected in the modeling. Since the overall potential change is not much, it shows that the accuracy of the finite element model is still high, and the stress value of the top plate calculated by ANSYS is not much different from the actual value, which is more reasonable, and the model can be used to analyze the shear hysteresis effect of the rigid-frame bridges and the force analysis.

Table 1: Stress detection and finite element calculation of cross section

Measuring point	Section position (m)	Measured stress at midpoint (Mpa)	Midpoint calculation stress (Mpa)	Error rate (%)
1	0	3.63	2.96	18.46%
2	11.5	-1.83	-1.54	15.62%
3	23	-6.85	-6.03	12.02%
4	34.5	-2.84	-3.71	30.84%
5	46	1.37	1.32	3.42%
6	57.5	6.25	5.48	12.36%
7	69	13.78	14.26	3.51%
8	80.5	10.45	10.59	1.38%
9	92	6.49	7.02	8.25%
10	103.5	3.92	3.59	8.44%
11	115	0.88	1.23	39.32%
12	126.5	-2.06	-1.58	23.46%
13	138	-5.31	-4.97	6.40%
14	149.5	-0.08	-0.03	64.66%
15	161	5.14	4.26	17.02%
16	172.5	1.99	2.67	33.62%
17	184	-0.91	-0.85	6.42%
18	195.5	-0.71	-1.03	44.45%

19	207	1.26	1.14	9.87%
20	218.5	3.34	3.24	3.13%
21	230	4.69	5.03	7.23%

III. B. Analysis of stress performance of key nodes of Rigid-Frame Bridge

III. B. 1) Design of bridge loading conditions

In this paper, energy variational method and finite element analysis model are applied to analyze the stresses of the case stiffened bridge. Due to the complexity of the bridge model and the large amount of computational data, it is necessary to select some key cross sections. The main girder side 1/2 cross-section and middle 1/2 cross-section are selected for analysis, and the cross-section is denoted as J1 and J2 in turn. The bridge belongs to the first-class highway and urban trunk road, which is a bidirectional 4-lane road, and this study designs two kinds of loading combinations of simulation conditions according to the design vehicle of the bridge, combined with the actual operation of the bridge in various situations. The simulated conditions are shown in Fig. 1, (a) and (b) represent condition 1 and condition 2, respectively, and the shaded part of the figure indicates that the lanes are loaded. Case 1 is the case where all lanes and sidewalks of the bridge are loaded, and Case 2 is the case where two lanes and two sidewalks are loaded.

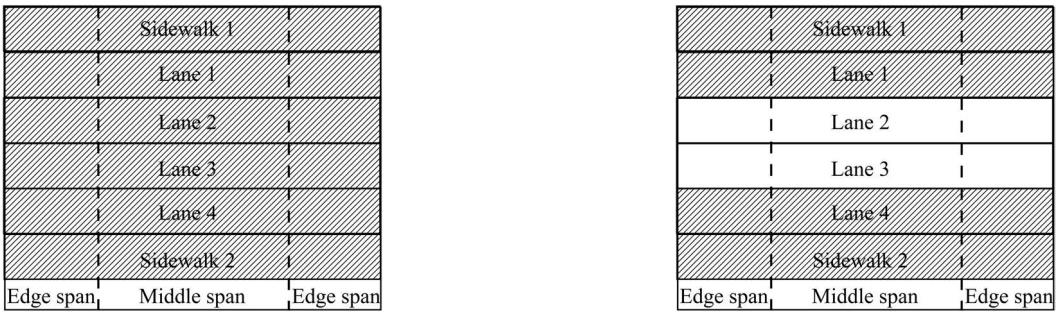

(a) Operating condition 1 (b) Operating condition 2

Figure 1: Operating condition

III. B. 2) Bridge force finite element analysis results

(1) Analysis of the stress performance of the top and bottom plates of J1 section (side span 1/2 section)

According to the ANSYS spatial finite element model, the positive stresses and shear hysteresis coefficients of the top and bottom plates of J1 section are calculated as shown in Fig. 2, (a) and (b) represent the results of the stress analysis of the top and bottom plates of J1 section, respectively, and (c) and (d) represent the results of the shear hysteresis coefficients analysis of the top and bottom plates of J1 section, respectively. In the figure, the X-axis is the cross-bridge direction of the main girder section, and X=0 indicates the center axis of Rigid-Frame Bridge girder. Under the symmetric loading condition, the positive stresses in the top and bottom plates are symmetrically distributed centered on the central axis of the bridge (X=0 m), but their lateral distribution is not uniform. the positive stresses in the top and bottom plates under the two conditions fluctuate in the web, and the maximum values of the bending positive stresses in the top and bottom plates appear in the middle web of the steel bridge (X=±1.1 m or so). With the increase of symmetric loading, the bending positive stresses in the top plate of J1 section roughly show an increasing trend, and the change of the bottom plate is not obvious. The maximum positive bending stresses in the top plate for Case 1 and Case 2 are -21.42 MPa and -20.13 MPa, respectively, and the maximum positive bending stresses in the bottom plate for Case 1 and Case 2 are -24.81 MPa and -24.80 MPa, respectively, from the results of shear hysteresis coefficient, the shear hysteresis coefficients of the top and bottom plates of the J1 cross-section are larger than that of Case 2 within the range of the mid-web plate for Case 1, indicating that the top and bottom plates of the J1 cross-section are more stressed than that of Case 2 with the increase of the symmetric load. This indicates that the shear hysteresis effect of the top and bottom plates of the J1 section in the range of the center web increases with the increase of symmetric load. The shear hysteresis coefficients show that the top and bottom plates of the critical node section of Rigid-Frame Bridge show obvious shear hysteresis phenomena, and the top and bottom plate shear hysteresis coefficients under the two conditions fluctuate in the web, and the serious location of the top plate shear hysteresis phenomenon under the two conditions appears in the vicinity of the mid-web plate of the steel bridge (X=±1.3m). The maximum shear hysteresis coefficients of the

top plate of the J1 section steel bridge under conditions 1 and 2 are 1.77 and 1.52, respectively, and their corresponding maximum shear hysteresis coefficients of the bottom plate are 3.61 and 3.43, respectively.

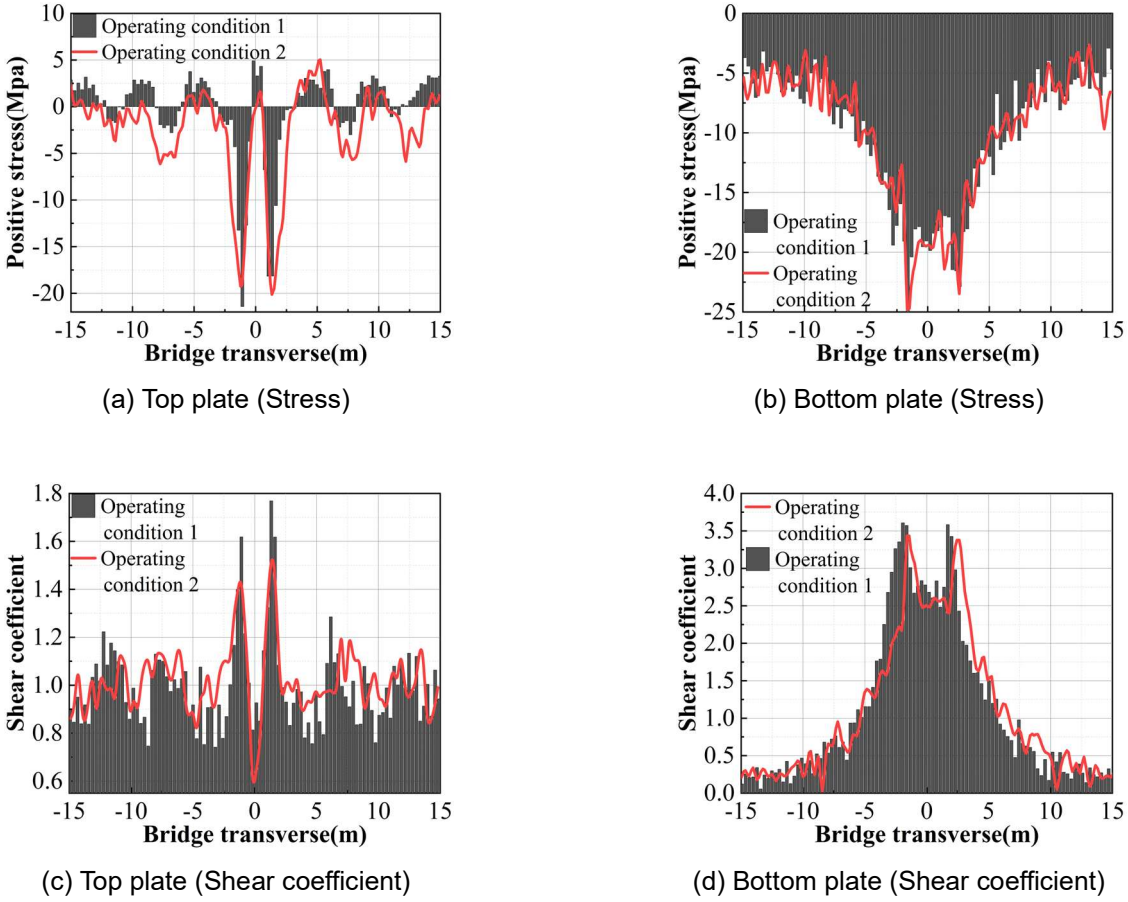

(a) Top plate (Stress)

(b) Bottom plate (Stress)

(c) Top plate (Shear coefficient)

(d) Bottom plate (Shear coefficient)

Figure 2: J1 force analysis results

(2) Analysis of stresses on top and bottom plates of J2 section (1/2 section of center span)

The results of positive stress and shear hysteresis coefficient analysis of the top and bottom plates of J2 section of Rigid-Frame Bridge are shown in Fig. 3, (a) and (b) represent the stress analysis results of the top and bottom plates of J2 section, and (c) and (d) represent the results of the shear hysteresis coefficient analysis of the top and bottom plates of J2 section, respectively. Under the symmetric loading condition of the main girder, the positive stresses in the top and bottom plates are symmetrically distributed centered on the central axis of the bridge (X=0m), but their transverse distributions are not uniform, and the positive stresses in the top and bottom plates fluctuate in the webs under the two conditions. The maximum bending positive stresses in the bottom plate under Case 1 and Case 2 were -34.25 MPa and -32.23 MPa, respectively, and the shear hysteresis coefficients indicated that the top and bottom plates of the steel bridges showed obvious shear hysteresis phenomena, and the top and bottom shear hysteresis coefficients fluctuated in the webs under the two cases. The maximum shear hysteresis coefficients of the top plate of the J2 section steel bridge under conditions 1 and 2 are 1.50 and 1.53, respectively, and the corresponding maximum shear hysteresis coefficients of the bottom plate are 8.01 and 8.54, respectively.

III. C. Optimized design analysis of Rigid-Frame Bridge force performance

In order to optimize the force performance of rigid-frame bridges, this section further investigates the force performance of rigid-frame bridges under different inclinations of box girder webs to provide reference ideas for the optimized design of rigid-frame bridges. Under the action of constant load, the length of the bottom plate of the original model of Rigid-Frame Bridge (inclination 90°) and the reduction of the length of the bottom plate by 30cm (inclination 60°) and 60cm (inclination 45°) on the basis of the original model are taken for the three cases of finite element analysis, respectively. The key node J1 and J2 sections of Rigid-Frame Bridge are selected and analyzed as represented by the change of shear hysteresis coefficient of the top plate of the key node section. When changing the inclination of the box girder web of Rigid-Frame Bridge, the results of the analysis of the shear hysteresis

coefficient of the top plate of the J1 section are shown in Table 2, and the results of the change of the shear hysteresis coefficient of the top plate of the J2 section are shown in Table 3. When the web inclination of Rigid-Frame Bridge is changed from 90° to 60° and 45°, the maximum shear hysteresis coefficient of the top plate of J1 section is changed from 1.079 to 1.060 and 1.046, which is gradually decreasing, and all of them appear at the junction of the ribs of the top plate. The simulation results from J2 section also show the same trend. When the inclination of the box girder web changes, it is a positive shear hysteresis effect, which indicates that the stress value at the junction of the top plate ribs in the J1 and J2 sections of the rigid frame bridge is larger than that in the middle of the top plate.

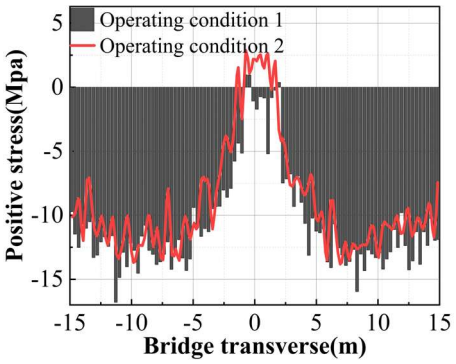

(a) Top plate (Stress)

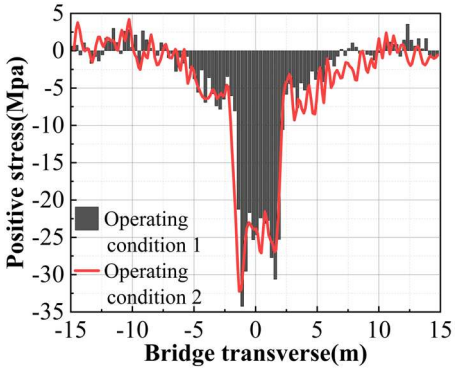

(b) Bottom plate (Stress)

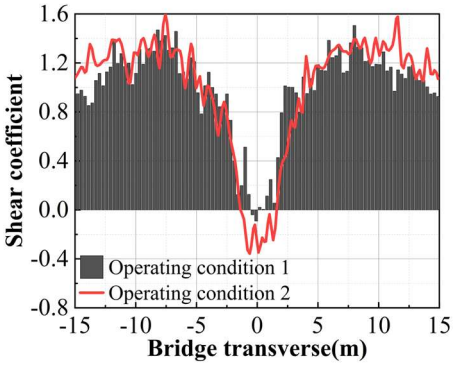

(c) Top plate (Shear coefficient)

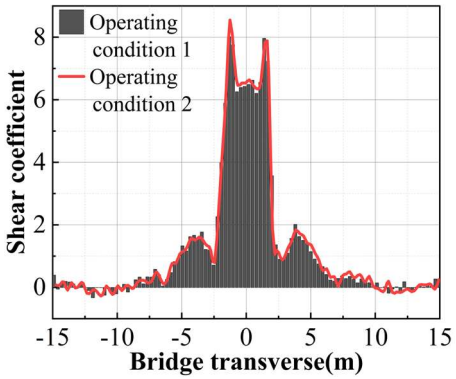

(d) Bottom plate (Shear coefficient)

Figure 3: J2 force analysis results

From the above analysis results, the web inclination of box girder of Rigid-Frame Bridge has some influence on the shear hysteresis effect of the bridge, so in the construction process of Rigid-Frame Bridge, it can be considered to increase the web inclination, so as to reduce the shear hysteresis effect of Rigid-Frame Bridge, to disperse the concentrated stress at the junction of the wing plate and the web plate, and to avoid transverse crack in the corresponding part, so as to realize the optimization of the structural design and safety of Rigid-Frame Bridge.

Table 2: Analysis of shear coefficient analysis(J1)

Top side (m)	The clinch of the plate		
	90°	60°	45°
-6	0.924	0.904	0.884
-5	0.973	0.952	0.937
-4	1.032	1.014	0.999
-3	1.065	1.048	1.031
-2	1.026	1.005	0.987
-1	0.984	0.958	0.943

0	0.955	0.935	0.920
1	0.992	0.972	0.960
2	1.043	1.026	1.005
3	1.079	1.060	1.046
4	1.038	1.021	1.005
5	0.981	0.964	0.939

Table 3: Analysis of shear coefficient analysis(J2)

Top side (m)	The clinch of the plate		
	90°	60°	45°
-6	1.085	1.066	1.039
-5	1.058	1.035	1.010
-4	1.017	0.999	0.968
-3	0.939	0.920	0.884
-2	0.993	0.964	0.937
-1	1.026	1.006	0.989
0	1.065	1.044	1.019
1	1.024	1.003	0.980
2	0.979	0.962	0.936
3	0.927	0.907	0.883
4	1.022	1.002	0.985
5	1.070	1.041	1.025

IV. Conclusion

This paper analyzes the shear hysteresis effect of Rigid-Frame Bridges using the energy-division method, and establishes a simulation model of the force performance of Rigid-Frame Bridges in the ANSYS program. The simulation validity verification found that the distribution trend of simulated and measured values is relatively consistent, and most of the values differ in size from 1.38% to 18.46% (15 measurement points). The influence of the mechanical performance of the key nodes of the rigid frame bridge and the inclination of the bridge web of the engineering case object is analyzed, and it is found that when all the lanes and sidewalks of the bridge are under load and 2 lanes and 2 sidewalks are loaded, the maximum bending normal stress of the roof of the J1 section of the key node is -21.42MPa and -20.13MPa, respectively, and the corresponding maximum bending normal stress of the bottom plate is -24.81MPa and -24.80MPa, respectively. The maximum shear hysteresis coefficients of the top plate of the J2-section steel bridge were 1.50 and 1.53, respectively, and their corresponding maximum shear hysteresis coefficients of the bottom plate were 8.01 and 8.54, respectively. It was also found that, when the inclination of the web plate of the stiffened bridge was changed from 90° to 60° and 45°, the maximum shear hysteresis coefficients of the top plate of the J1-section varied from 1.079 to 1.060 and 1.046, which was a gradual decrease, and all of them appeared at the junction of top plate ribs. This indicates that during the construction of Rigid-Frame Bridges, it can be considered to increase the inclination of the web plate, so as to reduce the shear hysteresis effect of Rigid-Frame Bridges, and realize the optimization of the structural design and safety of Rigid-Frame Bridges.

The analyses conducted in this study can clarify the force performance and shear hysteresis phenomenon of Rigid-Frame Bridges, and are of practical significance for ensuring and optimizing the structural safety of bridges.

References

[1] Dong, J. , Shan, D. , Zhang, E. , & Ma, T. . (2015). Seismic fragility of irregular continuous rigid frame bridge. Journal of Southwest Jiaotong University.

[2] Zhang, W. H. , Zhang, Y. T. , & Li, G. Q. . (2011). Evolutionary structural topology optimization for cantilever construction of continuous rigid-frame bridge. Applied Mechanics & Materials, 90-93, 18-22.

[3] Luo, C. , Lou, M. L. , & Gui, G. Q. . (2014). Comparing time history methods of input ground motion for large span continuous rigid frame bridge. Yantu Lixue/Rock and Soil Mechanics, 35, 414-422.

[4] Wang, W. F. , Zheng, G. Q. , Zhang, Z. L. , & Song, X. . (2011). Measuring and analysis of local stress under anchorage of continuous rigid frame bridge. Advanced Materials Research, 163-167, 1268-1273.

[5] Tang, X. Y. , Hu, Q. , & Yu, Y. H. . (2011). Seismic research of continuous rigid frame bridge under cantilever construction method. Advanced Materials Research, 368-373, 673-677.

[6] Liu, Z. , Li, Y. , Tang, L. , Liu, Y. , Jiang, Z. , & Fang, D. . (2014). Localized reliability analysis on a large-span rigid frame bridge based on monitored strains from the long-term shm system. Smart Structures & Systems, 14(2), 209-224.
[7] Li, Yinghua, Jiang, Zhenyu, Liu, & Yiping, et al. (2014). Localized reliability analysis on a large-span rigid frame bridge based on monitored strains from the long-term shm system. Smart Structures & Systems.
[8] Li, Y. , Tang, L. , Liu, Z. , & Liu, Y. . (2012). Statistics and probability analysis of vehicle overloads on a rigid frame bridge from long-term monitored strains. Smart Structures & Systems, 9(3), 287-301.
[9] Hu, Q. , Lin, B. , Xie, Y. , & Chen, W. . (2020). Study on mechanical performance of connection jointsin novel modular steel structure buildings. IOP Conference Series: Earth and Environmental Science, 605(1), 012015 (6pp).
[10] Jun, L. , Long-He, X. , & Xing-Si, X. . (2024). Seismic response characteristics and performance improvement of near-fault continuous rigid-frame bridges. Bulletin of earthquake engineering, 22(2), 731-755.
[11] Wei-Bo, S. , & Chun-Ning, Z. . (2012). Seismic analysis of tie beam of rigid frame bridge with high pier. Journal of Changan University.
[12] Sun, L. , Hao, X. W. , & Yang, Y. X. . (2011). Study on the optimization of depth-span ratio design for continuous rigid frame bridge girder. Advanced Materials Research, 280, 80-84.
[13] Wang, J. , & Sun, Q. . (2020). Parameter sensitivity analysis of stability of t -shaped rigid frame bridge by adopting swivel construction method. Multidiscipline Modeling in Materials and Structures, ahead-of-print(ahead-of-print).
[14] Song, X. M. , Melhem, H. , Cheng, L. J. , & Xu, Q. Y. . (2017). Optimization of closure jacking forces in multispan concrete rigid-frame bridges. Journal of bridge engineering, 22(3), 04016122.1-04016122.8.
[15] Song, X. , & Bai, L. . (2011). Mechanical characteristics analysis of pier-girder rigid node of continuous hybrid rigid frame railway bridge. Journal of Beijing Jiaotong University, 35(3), 77-80.
[16] Rojas, H. A. , Pezeshk, S. , & Foley, C. M. . (2012). Performance-based optimization considering both structural and nonstructural components. Earthquake Spectra, 23(3), 685-709.
[17] Liu, Z. . (2024). Innovative design of continuous rigid frame bridges with high piers and large spans in mountainous areas. Prestress Technology, 2(2), 58-69.
[18] Jie, L. I. , & Bin, C. . (2013). Analysis of continuous rigid frame bridge jacking force calculation and optimization. Journal of Zhengzhou University(Engineering Science).
[19] Wijaya, S. , & Rumintang, A. . (2021). The effect of truss modification and optimization on the performance of the new bridge sepanjang. CI-TECH.
[20] Xie, Y. , Yang, H. , Zuo, Z. , & Gao, Z. . (2019). Optimal depth-to-span ratio for composite rigid-frame bridges. Practice Periodical on Structural Design and Construction, 24(2), 05019001.1-05019001.8.
[21] Heng-Yang, S. , Jun, H. U. , & Yuan-Cheng, P. . (2015). Study of orthogonal test for design parameters of open-web continuous rigid-frame bridge. World Bridges.
[22] Hrvoje Vukoja,Anđelko Vlašić & Mladen Srbić. (2024). Shear Lag Effect on Box Steel Beams with Wide Curved Flanges. Applied Sciences(18),8481-8481.
[23] Yanfeng Li,Jiyuan Xie,Fengchi Wang,Di Wu,Jiahui Wang & Yanao Liu. (2024). Experimental Study on Shear Lag Effect of Long-Span Wide Prestressed Concrete Cable-Stayed Bridge Box Girder under Eccentric Load. Construction Materials(2),425-.
[24] Lasarzik Robert & Reiter Maximilian E. V. (2023). Analysis and Numerical Approximation of Energy-Variational Solutions to the Ericksen–Leslie Equations. Acta Applicandae Mathematicae(1).
[25] Emad Toma Karash,Muna Y. Slewa & Bushra Habeeb AL Maula. (2023). State Stress Analysis of Dental Restoration Materials Using the ANSYS Program. Revue des Composites et des Matériaux Avancés-Journal of Composite and Advanced Materials(3),183-192.